

Supporting Information

**A Low-cost Spiro[fluorene-9,9'-xanthene]-based Hole Transport
Material for Highly Efficient Solid-state Dye-sensitized Solar Cells
and Perovskite Solar Cells**

*Bo Xu,^{a, ‡} Dongqin Bi,^{b, ‡} Yong Hua,^a Peng Liu,^c Ming Cheng,^a Michael Grätzel,^d Lars Kloo,^c
Anders Hagfeldt,^{*, b} Licheng Sun^{*, a, e}*

^a Organic Chemistry, Center of Molecular Devices, Department of Chemistry, Chemical
Science and Engineering, KTH Royal Institute of Technology, SE-10044, Stockholm, Sweden.
E-mail: lichengs@kth.se

^b Laboratory of Photomolecular Science, Ecole Polytechnique Fédérale de Lausanne, CH-
1015, Lausanne, Switzerland. E-mail: anders.hagfeldt@epfl.ch

^c Applied Physical Chemistry, Center of Molecular Devices, School of Chemical Science and
Engineering, Department of Chemistry, KTH Royal Institute of Technology, SE-100 44,
Stockholm, Sweden.

^d Laboratory of Photonics and Interfaces, Ecole Polytechnique Fédérale de Lausanne, CH-
1015, Lausanne, Switzerland.

^e State Key Laboratory of Fine Chemicals, DUT-KTH Joint Research Center on Molecular
Devices, Dalian University of Technology (DUT), CN-116024, Dalian, China.

Experimental Section

Chemicals: 2,7-dibromo-9-fluorenone, 4-bromophenol, Methane sulfonic acid, 4,4'-dimethoxydiphenylamine, Sodium tert-butoxide, Tri-tert-butylphosphine, Palladium(II) acetate, 1,1,2,2-Tetrachloroethane (TeCA), Chlorobenzene (anhydrous 99.8%), acetonitrile (anhydrous 99.8%), Bis(trifluoromethane)sulfonimide lithium salt (Li-TSFI, 99.95%) and 4-tert-butylpyridine (t-BP, 96%) were purchased from Sigma-Aldrich. PbI_2 (purity 98%) and PbBr_2 (purity 99.999%) were purchased from TCI and Alfa, respectively. The t-BP was distilled before using; all of the other chemicals were used as received. Dye LEG4 and tris-(1H-pyrazol-1-yl)-4-tert-butylpyridine)cobalt(III) tris- (bis(trifluoromethyl sulfonyl)imide)) (FK209) was provided by Dyenamo AB. Spiro-OMeTAD was purchased from Luminescence Technology Corp. Solvents and other chemicals are also commercial available and used as received unless specially stated. Chromatography was performed using silica gel 60Å (35-63 μm). NMR spectra were recorded on a Bruker AVANCE 500 MHz spectrometer. High resolution MALDI spectra were collected with a Fourier transform-ion cyclotron resonance mass spectrometer instrument (Varian 7.0TFTICR-MS).

Synthesis of 2,2',7,7'-tetrabromospiro[fluorene-9,9'-xanthene] (4Br-SFX): A mixture of 4-bromophenol (17.3 g, 100 mmol), 2,7-dibromo-9-fluorenone (3.38 g, 10 mmol) and methane sulfonic acid (MeSO_3H , $d = 1.48 \text{ g/ml}$, 2.6 ml, 3.84 g, 40 mmol) was heated at 150 °C for 24 h. The reaction was cooled to room temperature, 100 ml methanol was slowly added into the mixture, then the white precipitate was filtered and washed with abundant of methanol, 5.9 g (yield 91 %) white powder was obtained. ^1H NMR (500 MHz, $(\text{CD}_3)_2\text{CO}$, 298 K), $\delta(\text{ppm})$: 8.00 (d, $J = 10 \text{ Hz}$, 2H), 7.69 (d, $J = 10 \text{ Hz}$, 2H), 7.48 (d, $J = 10 \text{ Hz}$, 2H), 7.43 (s, 2H), 7.30 (d, $J = 10 \text{ Hz}$, 2H), 6.53 (s, 2H).

Synthesis of $\text{N}_2, \text{N}_2', \text{N}_7, \text{N}_7'$ -octakis(4-methoxyphenyl)spiro[fluorene-9,9'-xanthene]-2,2',7,7'-tetraamine (X60): The synthesis of compound X60 was obtained by

Buchwald-Hartwig reaction in which 4,4'-dimethoxydiphenylamine (1.52 g, 6.62 mmol), **4Br-SFX** (1.0 g, 1.54 mmol), NaOtBu (0.74 g, 7.7 mmol), was added to 30 ml of dry toluene. The system was purged with nitrogen several times. Then P(t-Bu)₃ (0.03 g, 0.124 mmol), Pd(OAc)₂ (0.03 g, 0.124 mmol) was placed in mixture solution and reaction was refluxed overnight. Organic phase separation by ethyl acetate and combined organic phases were dried with MgSO₄ and purified with chromatography petroleum ether/ethyl acetate (1:1) to afford 1.57 g (yield 82%) of **X60**. ¹H NMR (500 MHz, *d*₆-DMSO, 298 K), δ (ppm): 7.35 (d, *J* = 10 Hz, 2H), 6.99 (d, *J* = 10 Hz, 2H), 6.85~6.67 (m, 34H), 6.60 (d, *J* = 10 Hz, 2H), 6.54 (s, 2H), 6.07 (s, 2H), 3.71 (s, 12H, OMe), 3.67 (s, 12H, OMe). ¹³C NMR (500 MHz, *d*₆-DMSO, 298 K), δ (ppm): 155.48, 154.89, 154.30, 147.44, 145.60, 143.36, 140.56, 140.13, 131.59, 125.97, 125.21, 124.66, 122.66, 120.23, 120.01, 119.84, 117.33, 116.00, 114.76, 114.64, 55.19, 55.18, 53.92. HR-MS (ESI) *m/z*: [M+1]⁺ calcd for 1240.4986; found, 1241.5033.

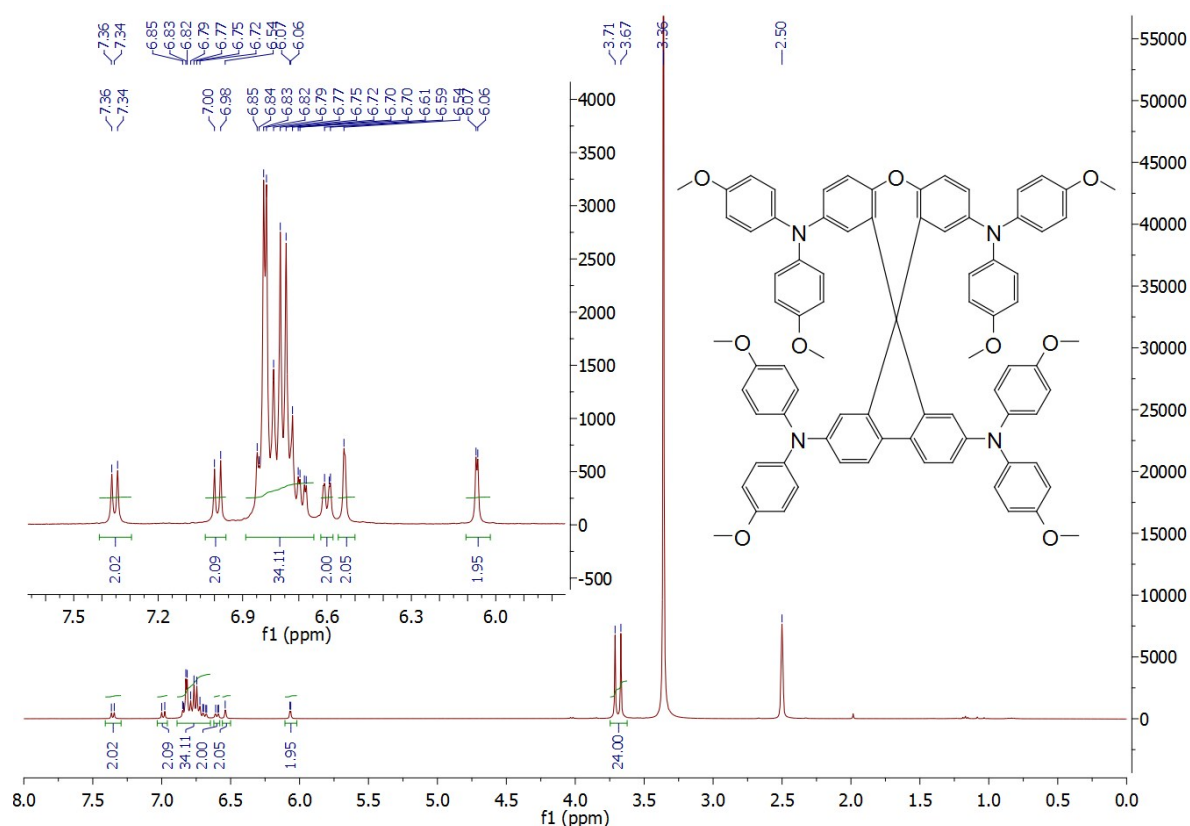


Figure S1. ¹H NMR (*d*₆-DMSO) spectrum of **X60**.

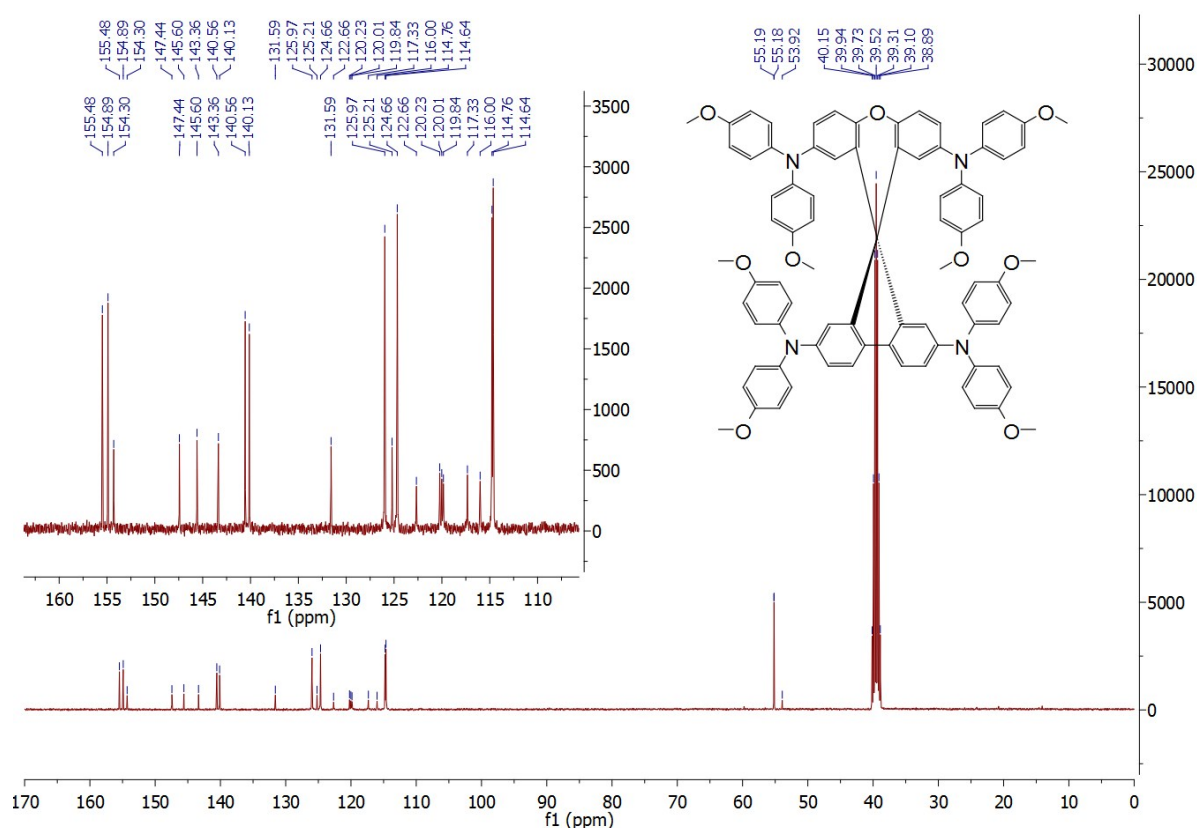


Figure S2. ^{13}C NMR (d_6 -DMSO) spectrum of **X60**.

Optical Characterization

UV-Vis absorption spectra were recorded on a Lambda 750 UV-Vis spectrophotometer. The fluorescence spectra of dye solutions were recorded on a Cary Eclipse fluorescence spectrophotometer. All samples were measured in a 1 cm cell at room temperature.

Electrochemical Measurements

Electrochemical experiments were performed with a CH Instruments electrochemical workstation (model 660A) using a conventional three-electrode electrochemical cell. A dichloromethane solution (DCM) containing 0.1 M of tetrabutylammoniumhexafluorophosphate ($n\text{-Bu}_4\text{NPF}_6$) was introduced as electrolyte, where an $\text{Ag}/0.01\text{ M AgNO}_3$ electrode (acetonitrile as solvent) was used as the reference electrode

and a glassy carbon disk (diameter 3 mm) as the working electrode, a platinum wire as the counter electrode. The cyclovoltammetric scan rates were 50 mV/s. All redox potentials were calibrated vs. normal hydrogen electrode (NHE) by the addition of ferrocene. The conversion $E_{(\text{Fc}/\text{Fc}^+)} = 630 \text{ mV vs NHE}$.

Computational Details

In the simulation, Optimization and single point energy calculations are performed using the cam-B3LYP¹ and the 6-31G** basis set for all atoms, without any symmetry constraints. All reported calculations were carried out by means of Gaussian 09². The reorganization energy λ , is determined by four energies, (the Nelson four-point method)^{3,4}:

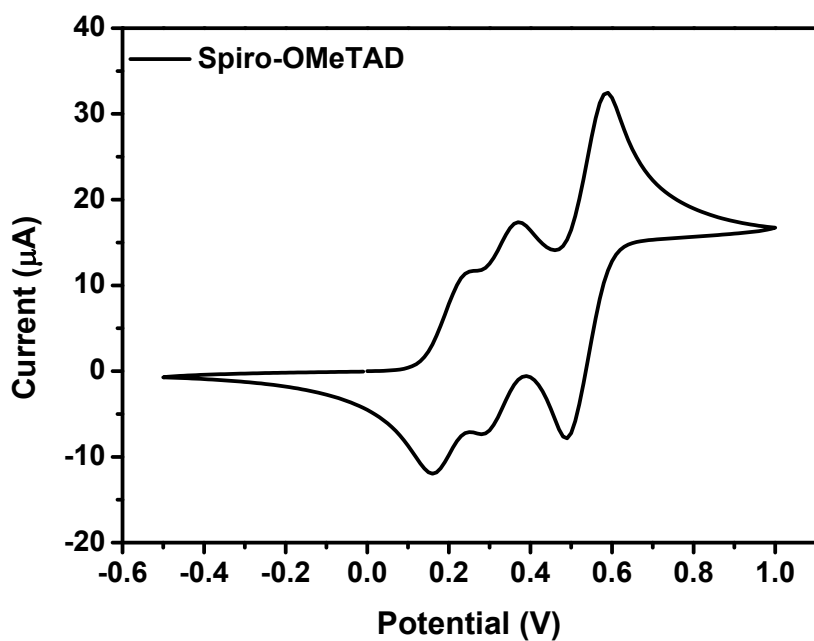
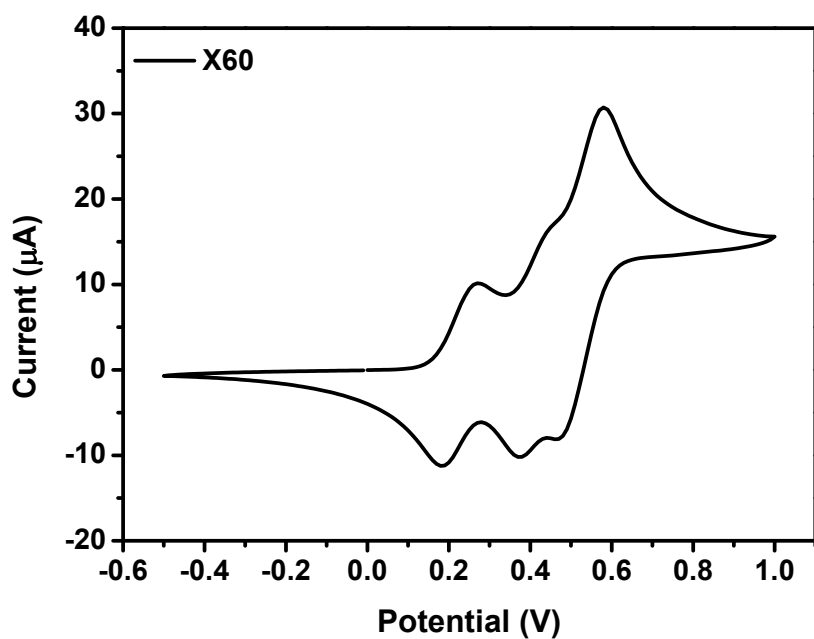
$$\lambda = E_+^* - E_+ + E^* - E$$

Where the E_+^* is the energy of the neutral molecule in the cation symmetry, and the E^* is the energy of the cationic molecule in the neutral symmetry; the E_+ and E are the optimized energies of the cationic and neutral molecules.

Non-adiabatic Marcus theory is used for calculate the charge transfer rate⁵, R:

$$R = \frac{2\pi}{\hbar} \frac{|J|^2}{\sqrt{4\pi\lambda k_B T}} e^{-\frac{(\Delta G_0 + \lambda)^2}{4k_B T}}$$

Where the λ is the reorganization energy, the J describes the electronic coupling, and ΔG_0 is the free energy between the equilibrium states of the products and reactants.



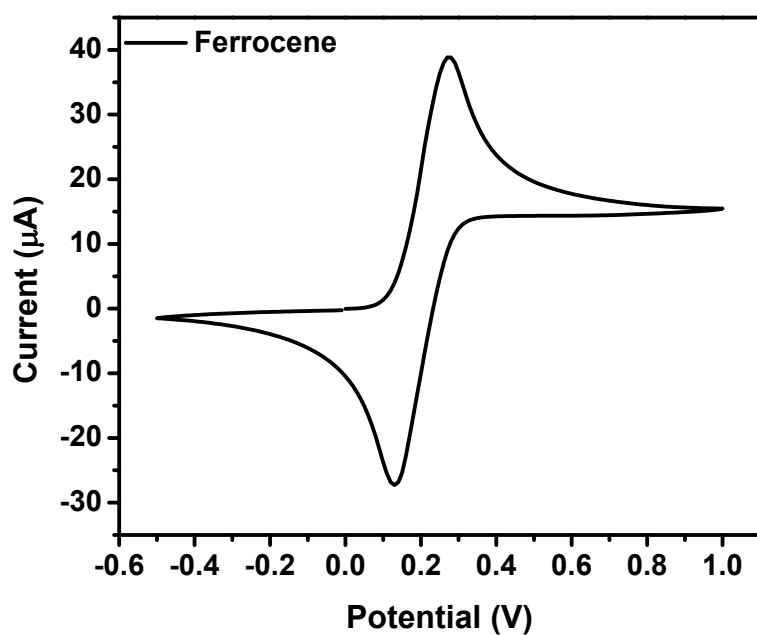


Figure S3. Cyclic voltammograms of **X60**, Spiro-OMeTAD and Ferrocene tested in DCM (10^{-4} M).

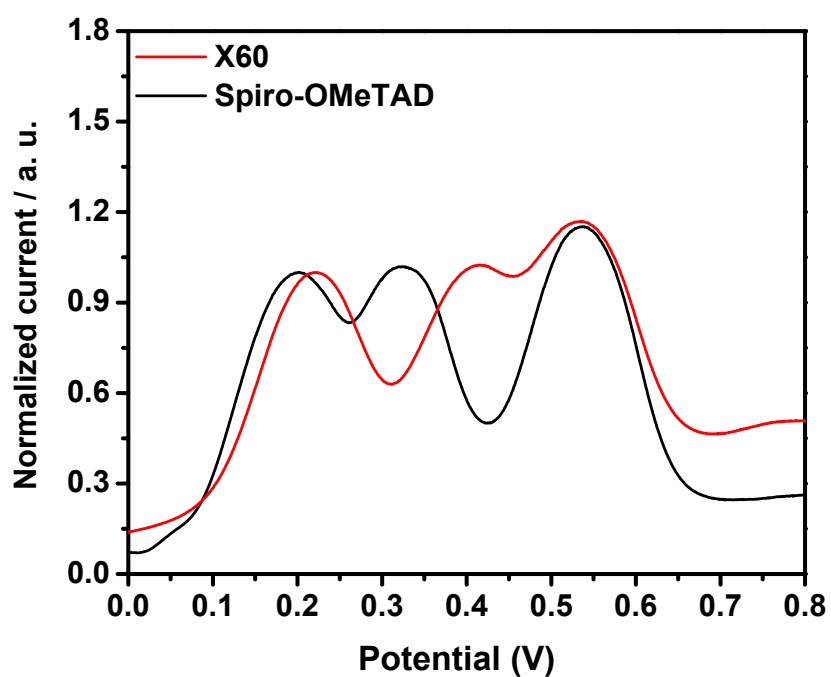


Figure S4. Normalized differential pulsed voltammetry (DPV) of **X60** and Spiro-OMeTAD in DCM (10^{-4} M).

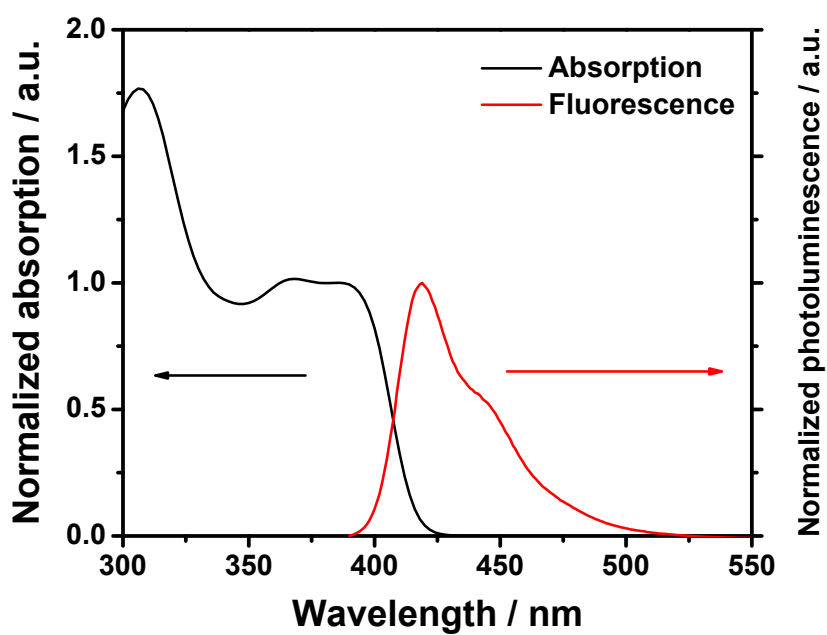


Figure S5. Normalized UV-Visible absorption and photoluminescence of **X60** in toluene (10^{-5} M).

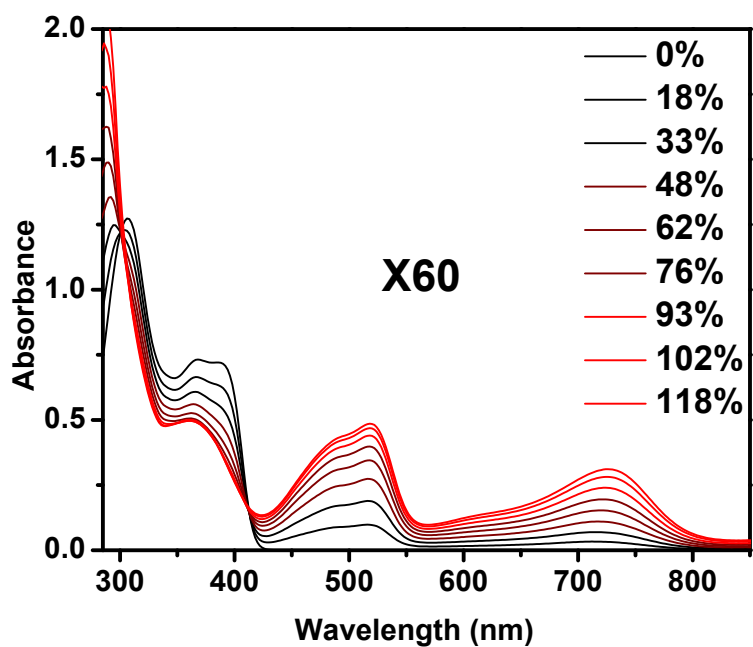


Figure S6. UV-vis absorption spectra of **X60** solution (2×10^{-5} M, in toluene) with the gradual addition of dopant-FK209.

Table S1. Summary of optical properties and band gap of HTM-X60 and Spiro-OMeTAD.

HTMs	λ_{abs} [nm]	λ_{em} [nm]	$E_{\text{o-o}}^{\text{a)}$ [eV]
X60	307	388	3.05
Spiro-OMeTAD	306	386	3.05

^{c)} Calculated from the intersection of the normalized absorption and emission spectra (Figure S5).

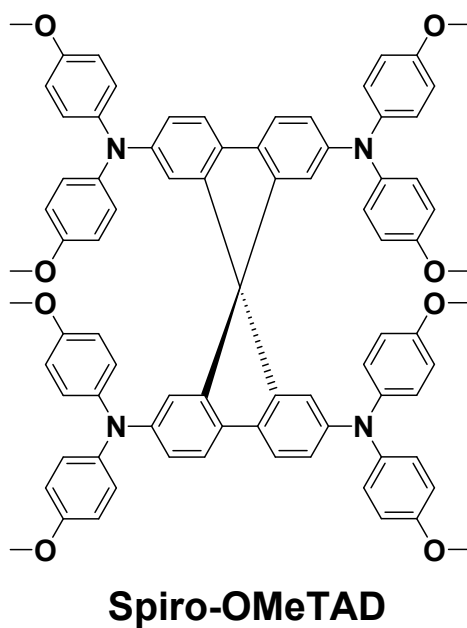
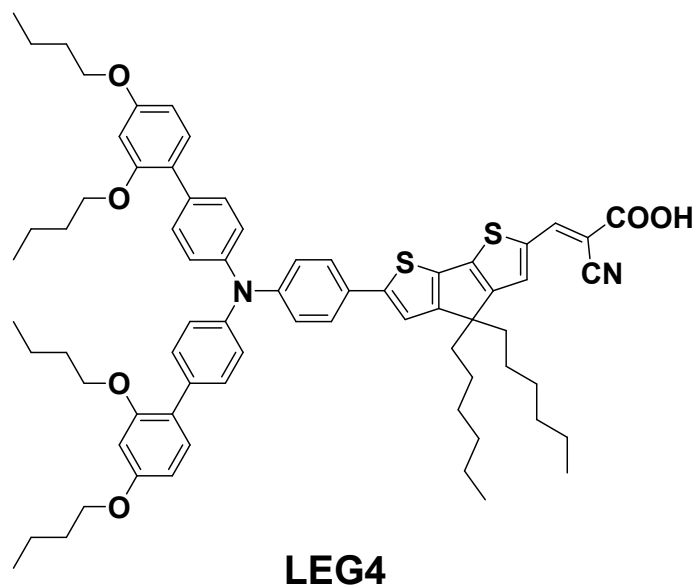


Figure S7. Molecular structures of LEG4 and Spiro-OMeTAD.

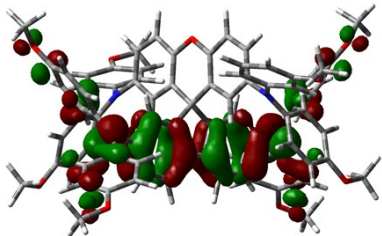
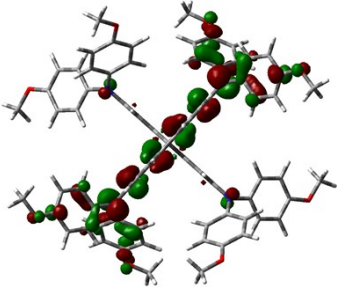
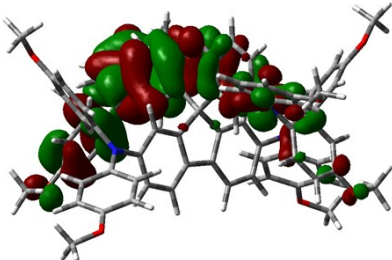
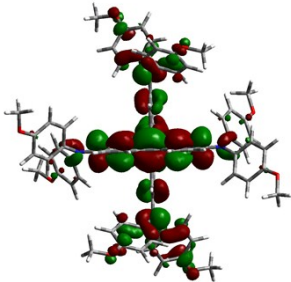
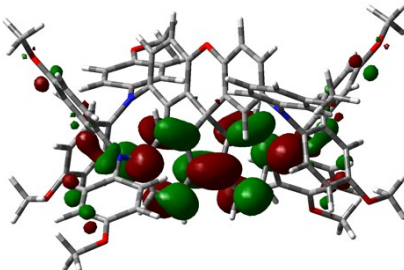
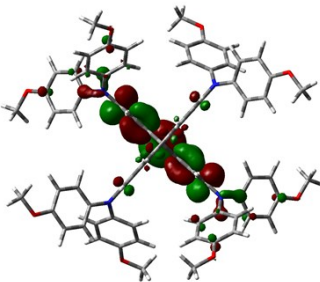
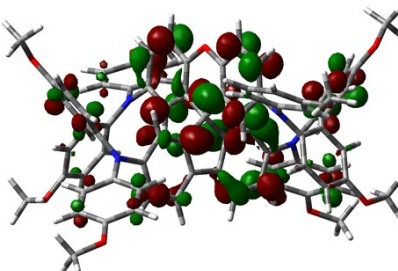
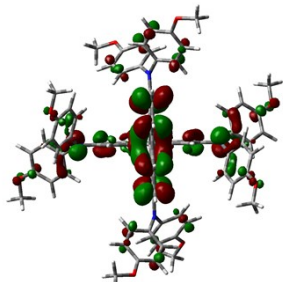
HTMs	X60	Spiro-OMeTAD
HOMO		
HOMO-1		
LUMO		
LUMO+1		

Figure S8. Frontier orbitals of **X60** and Spiro-OMeTAD.

Table S2. Calculated electrochemical properties of **X60** and Spiro-OMeTAD. Energy levels are given vs. vacuum.

HTMs	HOMO	HOMO-1	LUMO	LUMO-1
X60	-5.61	-5.49	0.48	0.84
Spiro-OMeTAD	-5.59	-5.45	0.47	0.62

Mobility Measurements

Hole mobility was investigated by the space-charge-limited current (SCLC) method, which can be described as the following equation:

$$J = \frac{9}{8} \mu \epsilon_0 \epsilon_r \frac{V^2}{d^3}$$

where J is the current density, μ is the hole mobility, ϵ_0 is the vacuum permittivity (8.85×10^{-12} F/ m), ϵ_r is the dielectric constant of the material (normally taken to approach 3 for organic semiconductors), V is the applied bias, and d is the film thickness. The hole-only devices were fabricated according to the literature.^{6,7}

Conductivity Measurements

The conductivities of the HTMs were determined by using a two-contact electrical conductivity set-up, which were performed by following a published procedure.⁶ Glass substrates without conductive layer were carefully cleaned in ultrasonic baths of detergents, deionized water, acetone and ethanol successively. Remaining organic residues were removed with 10 min by airbrushing. A thin layer of nanoporous TiO₂ was coated on the glass substrates by spin-coating with a diluted TiO₂ paste (Dyesol DSL 18NR-T) with terpineol (1:3, mass ratio). The thickness of the film is ca. 500 nm, as measured with a DekTak profilometer. After sintering the TiO₂ film on a hotplate at 500 °C for 30 min, the film was cooled to room temperature, before it was subsequently deposited by spin-coating of a solution of HTM in chlorobenzene, whereas the concentrations and additives were the same as in case of photovoltaic devices. Subsequently, a 200 nm thick Ag back contact was deposited onto the organic semiconductor by thermal evaporation in a vacuum chamber with a base pressure of

about 10^{-6} bar, to complete the device fabrication. J - V characteristics were recorded on a Keithley 2400 Semiconductor Characterization System.

Device Fabrication

Solid-state dye-sensitized solar cells:⁸ Fluorine-doped tin-oxide (FTO) coated glass substrates (Pilkington TEC15) were patterned by etching with zinc powder and 2 M hydrochloric acid. The substrates were carefully cleaned in ultrasonic baths of detergents, deionized water, acetone and ethanol successively. The remaining organic residues were removed with 10 min by airbrush. A compact TiO_2 blocking layer was deposited onto the surface of a pre-cleaned FTO substrate by spray pyrolysis on a hotplate at 450 °C using an airbrush. The solution used in the spray pyrolysis was 0.2 M Ti-isopropoxide, 2 M acetylacetone in isopropanol. In all electrode preparations 10 spray cycles were used as standard parameter. Nanoporous TiO_2 films were coated on the compact TiO_2 layer by screen-printing of a diluted TiO_2 paste (Dyesol DSL 18NR-T) with terpineol (2:1, mass ratio). The thickness of the film is ca. 2.5 μm , as measured with a DekTak profilometer. After sintering the TiO_2 film on a hotplate at 500 °C for 30 min, the film was cooled to room temperature and immersed in 0.02 M aqueous TiCl_4 at 70 °C for 30 min. The film was then rinsed by deionized water and then annealed on a hotplate at 500 °C for 30 min. After cooling to 90 °C, the film was immersed for 2 h in 0.1 mM solution of LEG4 dissolved in tert-butanol and acetonitrile (1:1), and then the sensitized electrodes were rinsed by ethanol and dried. Subsequently, the HTM solutions were prepared by dissolving the **X60** in chlorobenzene at a concentration of 150 mM, with addition of LiTFSI (20 mM, from a stock solution in acetonitrile with concentration of 0.5 M) and t-BP (200 mM, from a stock solution in chlorobenzene with concentration of 1.0 M). The HTM solution was left on the sensitized electrode for 30 s and then followed by spin-coating for 30 s with 2000 rpm. All of the HTM solutions were prepared in glove box under nitrogen atmosphere; chlorobenzene and

acetonitrile were deaerated by bubbling with dry nitrogen for half hours before introducing into glove box environment. The TeCA-doped HTM solutions (Doping with 4 % **TeCA**, volume ratio relative to chlorobenzene) were illuminated one minute for generation of the Spiro-OMeTAD⁺ by UV light ($\lambda=380$ nm) before spin coating. Subsequently, a 200 nm thick Ag back contact was deposited onto the organic semiconductor by thermal evaporation in a vacuum chamber with a base pressure of about 10^{-6} bar, to complete the device fabrication.

Perovskite solar cells: The devices of PSCs were fabricated according to a published method.⁹ The washing and etching procedures were the same as in case of ssDSC devices. A 20~30 nm TiO₂ blocking layer was deposited on the cleaned FTO glass by spray pyrolysis using O₂ as the carrying gas at 450°C from a precursor solution of 0.6 ml titanium diisopropoxide and 0.4 ml Acetylacetonate in 7 ml anhydrous Isopropanol. A 200 nm mesoporous TiO₂ was coated on the substrate by spin coating with a speed of 4500 rpm for 15 s with a ramp of 2000 rpm·s⁻¹, from a diluted 30 nm particle paste (Dyesol) in Ethanol, the weight ratio of TiO₂ (Dyesol paste) and Ethanol is 5.5:1. After that, the substrate was immediately dried on a hotplate at 80°C, and then the substrates were sintered at 500°C for 20 min. The perovskite film was deposited by spin coating onto the TiO₂ substrate. The perovskite layer was deposited by spin coating the perovskite precursor solution in one-step, which was prepared by mixing of the formamidinium iodide (FAI), lead iodide (PbI₂), methylammonium bromide (MABr) and lead bromide (PbBr₂) in a mixed solvent of DMF and DMSO solution (volume ratio 4:1) with the molar concentration of 1.35M Pb²⁺ (PbI₂ and PbBr₂). The molar ratio of PbI₂/PbBr₂=85/15, PbI₂/FAI=1.05, PbBr₂/MABr=1/1. The spin coating procedure was done in an Argon flowing glovebox, first 2000 rpm for 10 s with a ramp of 200 rpm·s⁻¹, second 6000 rpm for 30 s with a ramp of 2000 rpm·s⁻¹. 110 μ l chlorobenzene was dropped on the spinning substrate during the second spincoating step 20 s before the end of the procedure. The substrate was then heated at 100°C for 90 min on a

hotplate. After cooling down to room temperature, HTM was subsequently deposited on the top of the perovskite layer by spin coating at 3000 rpm for 20 s. The HTM solutions were prepared by dissolving the **X60** in chlorobenzene at a concentration of 60 mM, with the addition of 30 mM LiTFSI (from a stock solution in acetonitrile with concentration of 1.0 M), 200 mM of t-BP (from a stock solution in chlorobenzene with concentration of 1.0 M) and 1.8 mM FK209 (from a stock solution in acetonitrile with concentration of 0.5 M). The HTM solution was dripped on the perovskite electrode and then followed by spin-coating for 30 s with 3000 rpm. All of the HTM solutions were prepared in glove box under nitrogen atmosphere; chlorobenzene and acetonitrile were deaerated by bubbling with dry nitrogen for half hours before introducing into glove box environment. Finally, 80 nm of gold was deposited by thermal evaporation using a shadow mask to pattern the electrodes.

Device Characterization

Current-Voltage characteristics were recorded by applying an external potential bias to the cell while recording the generated photocurrent with a Keithley model 2400 digital source meter. The light source was a 300 W collimated xenon lamp (Newport) calibrated with the light intensity to $100 \text{ mW}\cdot\text{cm}^{-2}$ at AM 1.5 G solar light condition by a certified silicon solar cell (Fraunhofer ISE). IPCE spectra were recorded on a computer-controlled setup comprised of a xenon lamp (Spectral Products ASB-XE-175), a monochromator (Spectral Products CM110) and a Keithley multimeter (Model 2700). The setup was calibrated with a certified silicon solar cell (Fraunhofer ISE) prior to measurements. The prepared ssDSC samples were masked during the measurement with an aperture area of 0.126 cm^2 (diameter 4 mm) exposed under illumination. The prepared PSC samples were masked during the measurement with an aperture area of 0.16 cm^2 exposed under illumination.

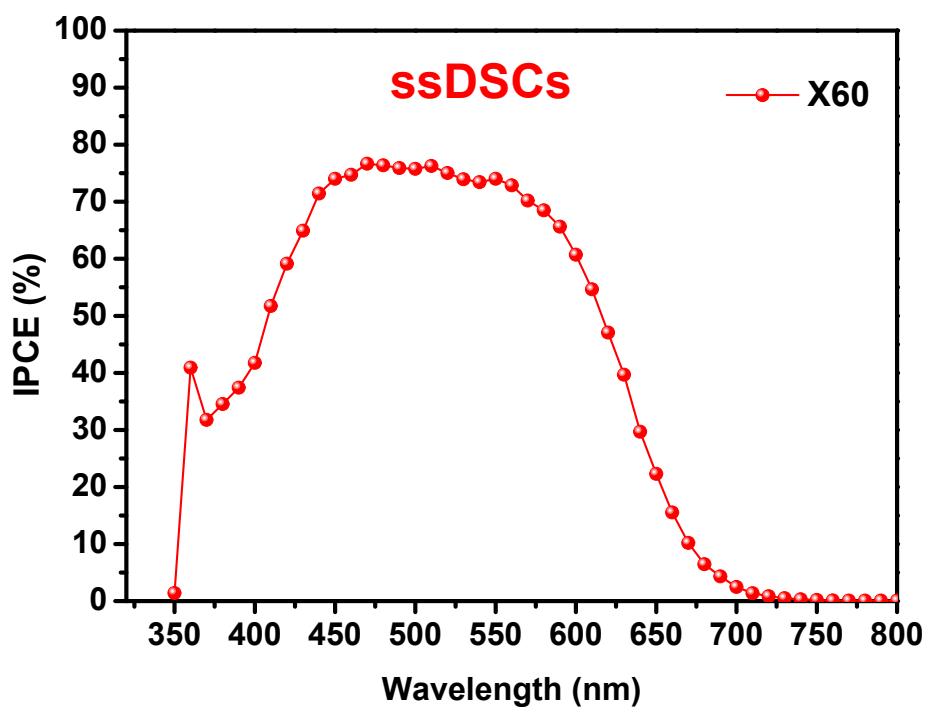


Figure S9. Corresponding IPCE spectrum of the X60-based ssDSCs.

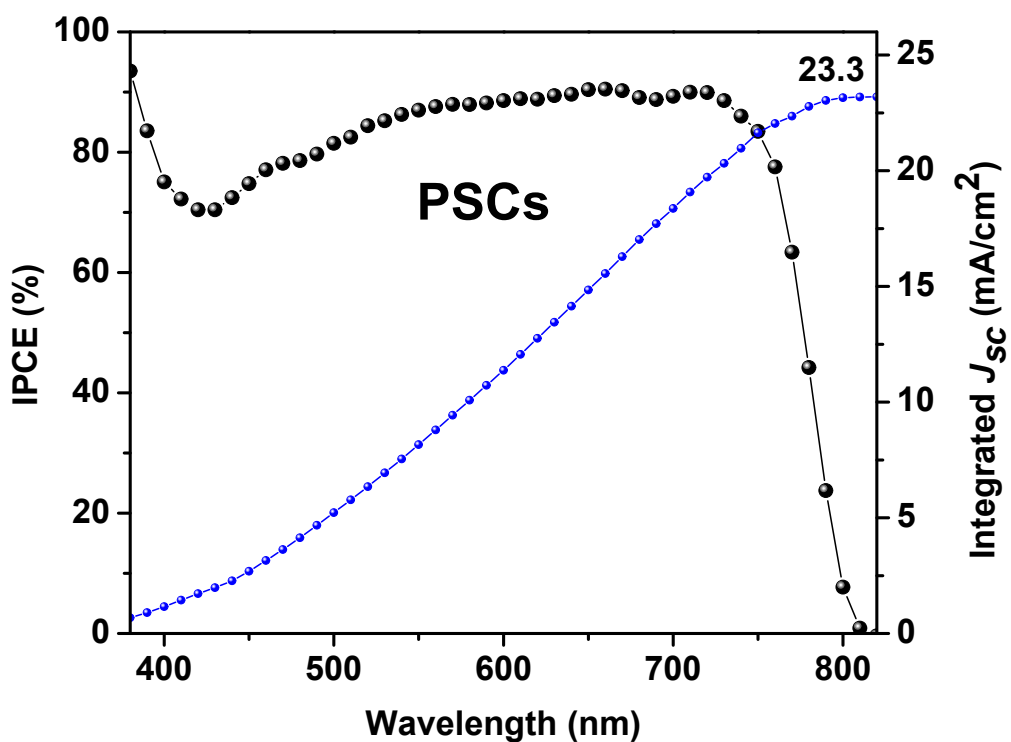


Figure S10. Corresponding IPCE spectrum of the X60-based PSCs.

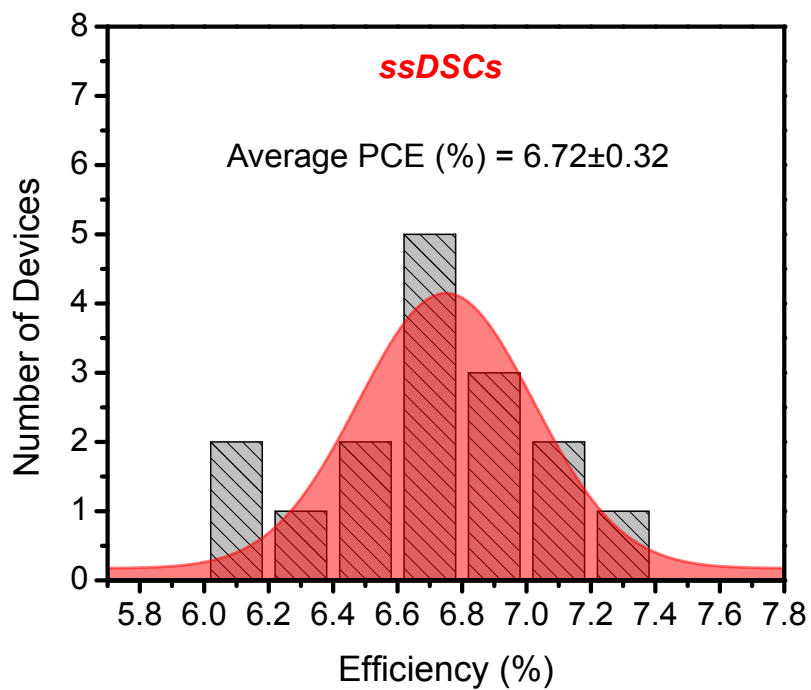


Figure S11. Histogram of ssDSCs efficiencies based on **X60** as HTM (at least 16 devices were studied).

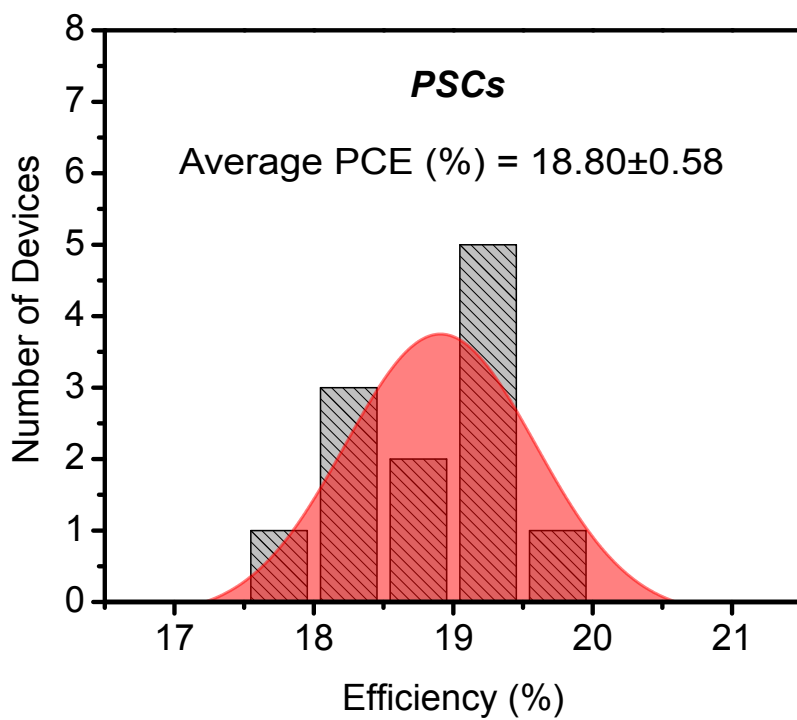


Figure S12. Histogram of PSCs efficiencies based on **X60** as HTM (at least 12 devices were studied).

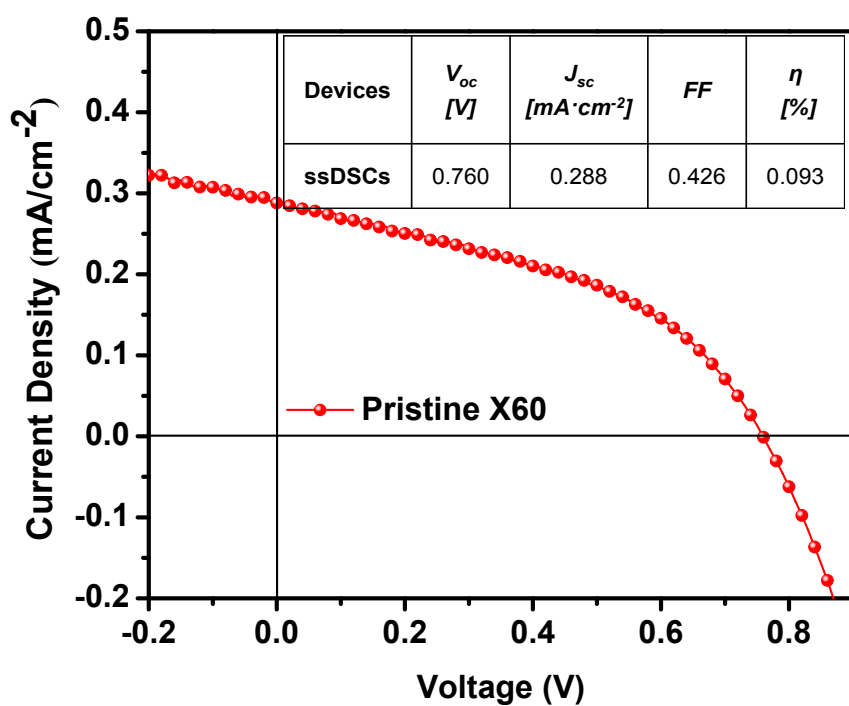


Figure S13. J - V characteristic of pristine **X60** based ssDSCs, which were measured under 100 $\text{mW}\cdot\text{cm}^{-2}$ AM1.5G solar illumination.

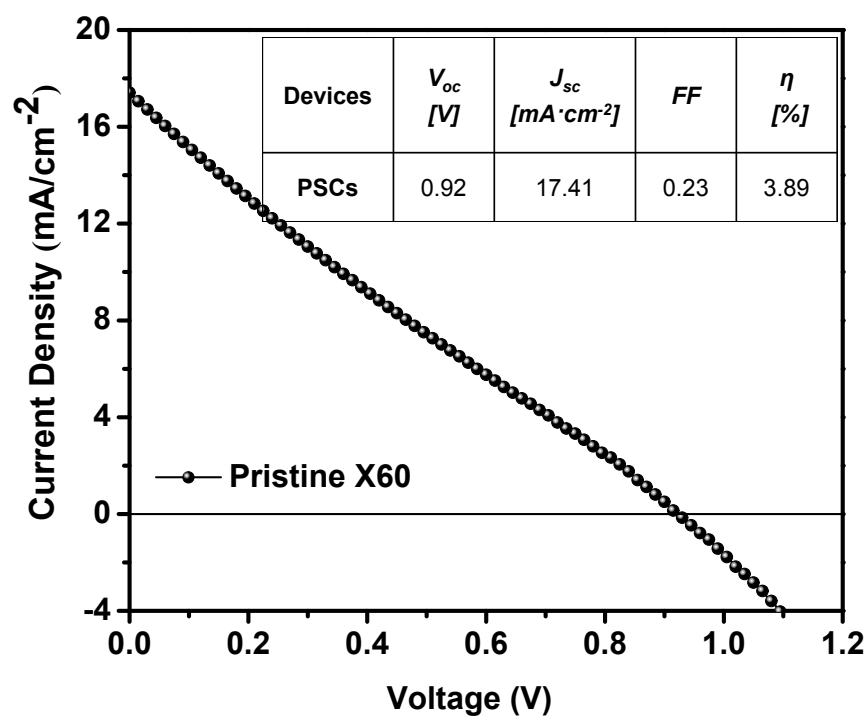


Figure S14. J - V characteristic of pristine **X60** based PSCs, which were measured under 94.7 $\text{mW}\cdot\text{cm}^{-2}$ solar illumination.

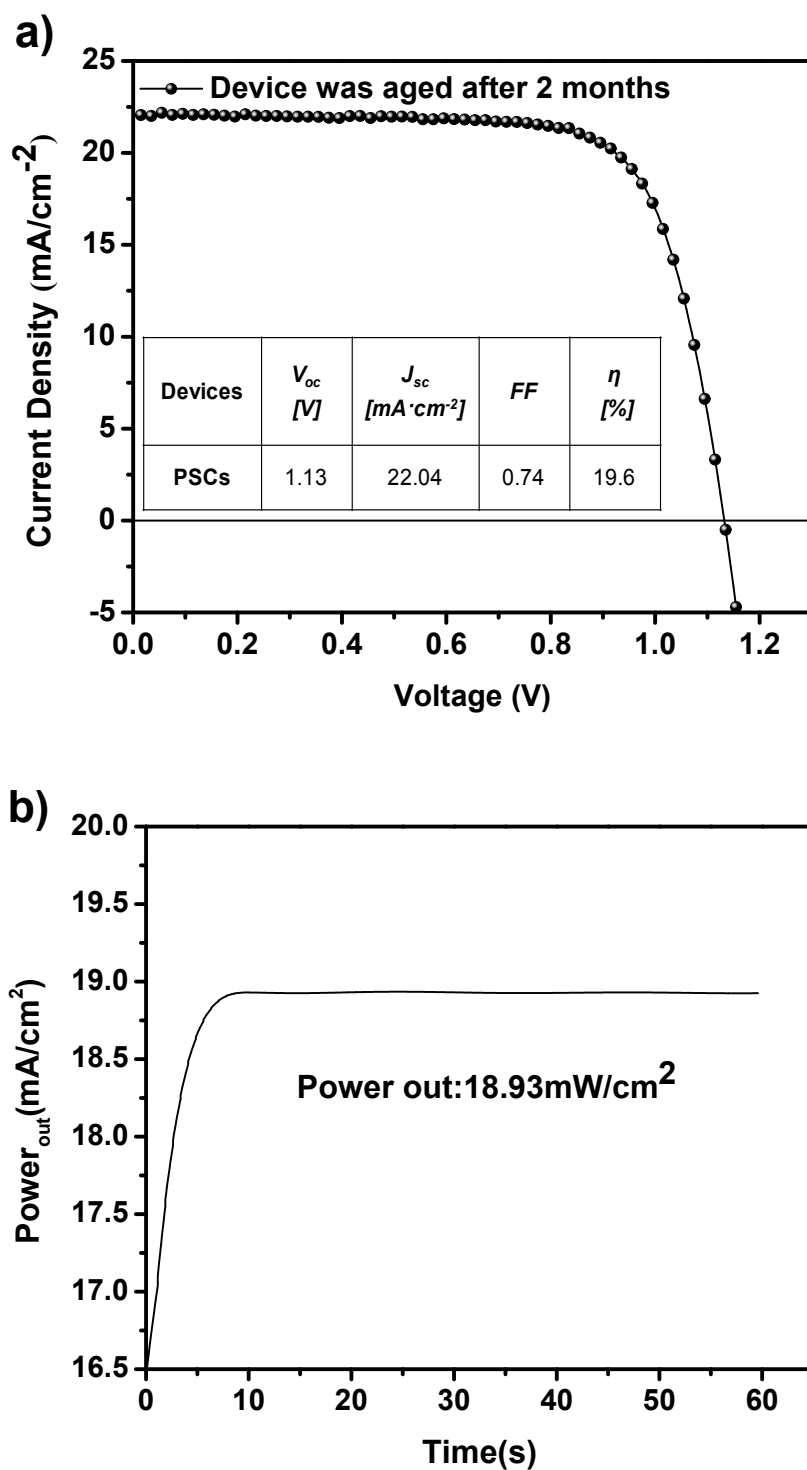


Figure S15. a) J - V characteristic of a **X60** based PSC after stored in desiccator in the dark for two months (the devices was sealed by using the epoxy and measured under $94.7 \text{ mW}\cdot\text{cm}^{-2}$ solar illumination). b) Stabilized power output of the same device that measured over one minute.

Synthesis cost estimation of 1 gram 4Br-SBF and 4Br-SFX.

We roughly estimated the synthesis cost of 1 gram 4Br-SBF and 4Br-SFX according to the cost model that was described by Pablo *et al.*¹⁰ and Osedach *et al.*¹¹ The quotes (for bulk quantities when possible) have been collected from major chemical suppliers (Sigma-Aldrich, Alfa, TCI and Fischer) for all used chemicals. The estimated synthesis cost of 4Br-SFX (1.12 \$/g) is 30 times lower than that of the 4Br-SBF (33.89 \$/g). (**Figure S13 and S14, Table S3 and S4**).

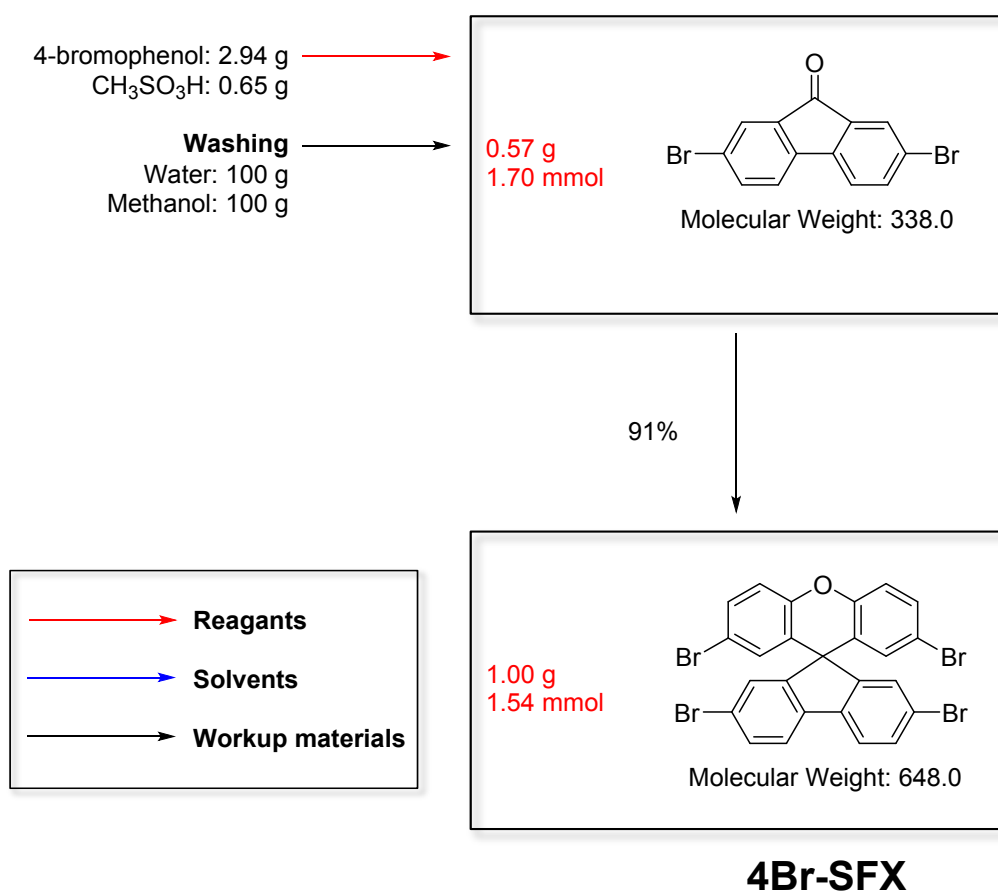


Figure S16. Synthetic routes 1 gram of 4Br-SFX.

Table S3: Materials quantities and cost for the synthesis of 4Br-SFX.

Chemical name	Weight reagent (g)	Weight solvent (g)	Weight workup (g)	Price of Chemical (\$/kg)	Material cost (\$/g product)	Cost per step (\$/step)
2,7-dibromo-9-fluorenone	0.57 g			421.00	0.24	1.12
4-bromophenol	2.94 g			203.78	0.60	
Methane sulfonic acid	0.65 g			85.21	0.06	
Methanol			100 g	2.21	0.22	
Water			100 g	-	-	
Total	4.16 g		200 g			1.12 \$/g

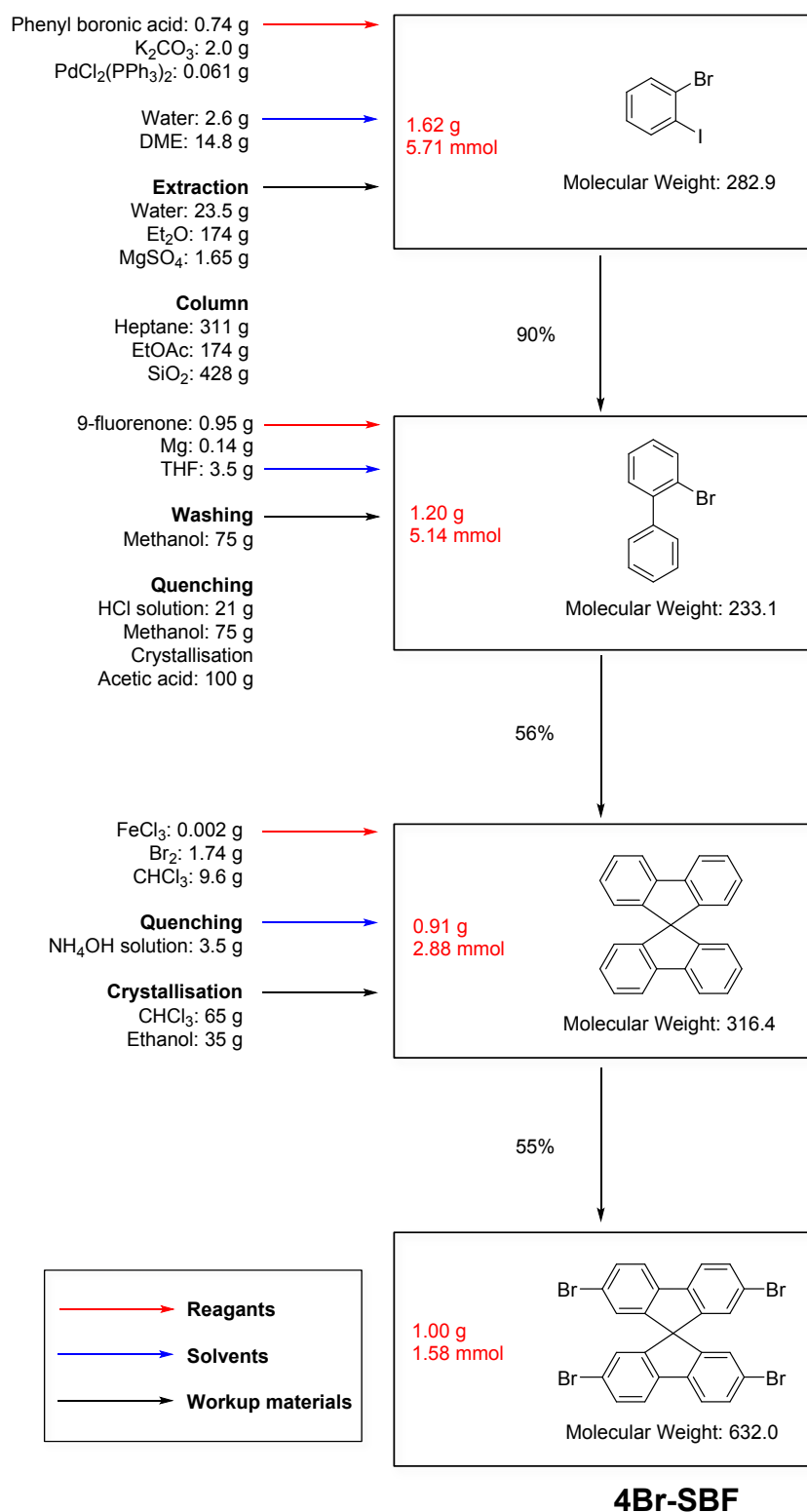


Figure S17. Synthetic routes of 1 gram of 4Br-SBF.¹⁰

Table S4: Materials quantities and cost for the synthesis of 4Br-SBF.¹⁰

Chemical name	Weight reagent (g)	Weight solvent (g)	Weight workup (g)	Price of Chemical (\$/kg)	Material cost (\$/g product)	Cost per step (\$/step)
Phenylboronic acid	0.74 g			1419.73	1.05	28.63
K ₂ CO ₃	2.0 g			6.74	0.02	
PdCl ₂ (PPh ₃) ₂	0.061 g			16,701.4	1.02	
Water		2.6 g		-	-	
Dimethoxyethane		14.8 g		94.77	1.40	
Water			23.5 g	-	-	
Diethyl ether			174 g	22.89	3.98	
MgSO ₄			1.65 g	54.24	0.09	
Heptane			311 g	4.59	1.43	
Ethyl acetate			174 g	3.63	0.63	
Silica gel			428 g	44.41	19.01	
9-Fluorenone	0.95 g			162.72	0.15	4.62
Magnesium	0.14 g			36.32	0.01	
Tetrahydrofuran		3.5 g		9.94	0.04	
Methanol			75 g	2.21	0.17	
Hydrochloric acid (5%)			21 g	3.13	0.07	
Methanol			75 g	2.21	0.17	
Acetic acid			100 g	40.12	4.01	
Iron(III) chloride	0.002 g			17.09	0	0.64
Bromine	1.74 g			44.33	0.08	
Chloroform		9.6 g		2.6	0.03	
NH ₄ OH (25%)			3.5 g	8.14	0.03	
Chloroform			65 g	2.6	0.17	
Ethanol			35 g	9.53	0.33	
Total	5.633 g	30.5 g	1486.65 g	-	-	33.89 \$/g

References

- (1) Becke, A. D. *The Journal of Chemical Physics* **1993**, 98, 1372.
- (2) Frisch, M. J.; Trucks, G. W.; Schlegel, H. B.; Scuseria, G. E.; Robb, M. A.; Cheeseman, J. R.; Scalmani, G.; Barone, V.; a, B. M.; Petersson, G. A.; Nakatsuji, H.; Caricato, M.; and, X. L.; Hratchian, H. P.; Izmaylov, A. F.; Bloino, J.; Zheng, G.; Sonnenberg, J. L.; and H. Nakai and T. Vreven and Montgomery, {Jr.}, J. A. and J. E. Peralta and F. Ogliaro and M. Bearpark and J. J. Heyd and E. Brothers and K. N. Kudin and V. N. Staroverov and R. Kobayashi and J. Normand and K. Raghavachari and A. Rendell and J. C. Burant and S. S. Iyengar and J. Tomasi and M. Cossi and N. Rega and J. M. Millam and M. Klene and J. E. Knox and J. B. Cross and V. Bakken and C. Adamo and J. Jaramillo and R. Gomperts and R. E. Stratmann and O. Yazyev and A. J. Austin and R. Cammi and C. Pomelli and J. W. Ochterski and R. L. Martin and K. Morokuma and V. G. Zakrzewski and G. A. Voth and P. Salvador and J. J. Dannenberg and S. Dapprich and A. D. Daniels and Ö. Farkas and J. B. Foresman and J. V. Ortiz and J. Cioslowski and D. J. Fox, M. H. a. M. E. a. K. T. a. R. F. a. J. H. a. M. I. a. T. N. a. Y. H. a. O. K. **Gaussian Inc. Wallingford CT 2009**.
- (3) Lee, C.; Waterland, R.; Sohlberg, K. *Journal of Chemical Theory and Computation* **2011**, 7, 2556.
- (4) Nelsen, S. F.; Blackstock, S. C.; Kim, Y. *Journal of the American Chemical Society* **1987**, 109, 677.
- (5) Marcus, R. A.; Sutin, N. *Biochimica Et Biophysica Acta* **1985**, 811, 265.
- (6) Snaith, H. J.; Gratzel, M. *Appl. Phys. Lett.* **2006**, 89, 262114.
- (7) Xu, B.; Tian, H.; Lin, L.; Qian, D.; Chen, H.; Zhang, J.; Vlachopoulos, N.; Boschloo, G.; Luo, Y.; Zhang, F.; Hagfeldt, A.; Sun, L. *Advanced Energy Materials* **2014**, n/a.
- (8) Xu, B.; Tian, H.; Bi, D.; Gabrielsson, E.; Johansson, E. M. J.; Boschloo, G.; Hagfeldt, A.; Sun, L. *Journal of Materials Chemistry A* **2013**, 1, 14467.
- (9) Bi D; Tress W; Dahr I; Gao P; Luo J; Renevier C; Schenk K; Abate A; Giordano F; Beana J; Decoppet J; Zakeeruddin S. M.; Nazeeruddin M. K.; Grätzel M; Hagfeldt A *Science Advances* **2015**, Will be online soon.
- (10) Petrus, M. L.; Bein, T.; Dingemans, T. J.; Docampo, P. *Journal of Materials Chemistry A* **2015**, 3, 12159.
- (11) Osedach, T. P.; Andrew, T. L.; Bulovic, V. *Energy & Environmental Science* **2013**, 6, 711.